

Large-scale Fading Decoding based Massive MIMO System with Regularized Zero Forcing Precoder

Fathima Zaheera¹, Dr. I. V. Prakash²

¹Assistant Professor, ²Professor, ^{1,2}Department of ECE

^{1,2}Gandhi Institute for Technology, Bhubaneswar, India

Abstract

In this paper, we study the uplink (UL) and downlink (DL) spectral efficiency (SE) of a cell-free massive multiple input-multiple-output (MIMO) system over Rician fading channels. The phase of the line-of-sight (LoS) path is modeled as a uniformly distributed random variable to take the phase-shifts due to mobility and phase noise into account. Considering the availability of prior information at the access points (APs), the regularized zero forcing (RZF) is developed and compared with phase-aware minimum mean square error (MMSE), non-aware linear MMSE (LMMSE), and least-square (LS) estimators are derived. The MMSE estimator requires perfectly estimated phase knowledge whereas the LMMSE and LS are derived without it. In the UL, a two-layer decoding method is investigated in order to mitigate both coherent and non-coherent interference. Closed form UL SE expressions with phase-aware proposed RZF, and existing MMSE, LMMSE, and LS estimators are derived for maximum-ratio (MR) combining in the first layer and optimal large-scale fading decoding (LSFD) in the second layer. In the DL, two different transmission modes are studied: coherent and non-coherent. Closed-form DL SE expressions for both transmission modes with RZF precoding are derived. Numerical results show that the RZF-LSFD improves the UL SE performance and coherent transmission mode performs much better than non-coherent transmission in the DL. Besides, the performance loss due to the lack of phase information depends on the pilot length and it is small when the pilot contamination is low.

Index Terms—Cell-free massive MIMO, Rician fading, phase shift, performance analysis.

I. INTRODUCTION

Cell-free massive MIMO refers to a distributed MIMO system with a large number of APs that jointly serve a smaller number of user equipment's (UEs) [2–5]. The APs cooperate via a fronthaul network [5] to spatially multiplex the UEs on the same time-frequency resource, using network MIMO methods that only require locally obtained channel state information (CSI) [6]. In its canonical form, cell-free massive MIMO uses MR combining because of its low complexity. Due to the fact that MR combining cannot suppress the interference well, some APs receive more interference from other UEs than signal power from the desired UE. The LSFD method is proposed in [7] and [8] to mitigate the interference for co-located massive MIMO systems. This method is generalized for more realistic spatially correlated Rayleigh fading channels with arbitrary first-layer decoders in [9], [10]. The two-layer decoding technique is first adapted to cell-free massive MIMO networks in [11] for a Rayleigh fading scenario. In the concurrent paper [12], the LSFD method is studied in a setup with Rician fading channels where the LoS phase is static. Joint transmission from multiple APs can be either coherent (same data from all APs) or non-coherent (different data). Only the former has been considered in cell-free massive MIMO, but it requires that the APs are phase-synchronized. A synchronization method is outlined in [5], [13], [14] without validation. In densely deployed systems, like cell-free massive MIMO, the channels typically consist of a combination of a semideterministic

LoS path and small-scale fading caused by multipath propagation, which can be modeled as Rician fading [12], [15]. A small change in the UE location may result in a significant phase-shift of the LoS component, but no change in amplitude. For instance, if the UE moves half a wavelength away from the AP, the phase of the channel response changes by $\pm\pi$. Similarly, hardware effects such as phase noise may create severe shift in the phase. These effects are usually neglected in the analysis of Rician fading channels by assuming a LoS path with static phase. Especially in high mobility scenarios, the phase shift in LoS path may have a large impact on system performance. Recently, [16] studied a cell-free network that supports both unmanned aerial vehicles (UAVs) and ground UEs where the channels between AP-UAV pairs have Rician distribution with uniformly distributed phase on the LoS paths. Each AP needs to learn the channel statistics of each UE that it serves, as well as the statistics of the combined interfering signals, if Bayesian channel estimators are to be used. The large-scale fading coefficients can be estimated with a negligible overhead since the coefficients are deterministic [17]; several practical methods to estimate these coefficients using uplink pilots are presented in [18]. However, the phase-shifts are harder to estimate since they change as frequently as the small-scale fading. Depending on the availability of channel statistics, the phase aware MMSE estimator which requires all prior information, LMMSE estimator with only the large-scale fading parameters, or LS estimator with no prior information can be utilized. In this paper, the specific technical contributions are as follows: We consider Rician fading channels between the APs and UEs, where the mean and variance are different for every AP-UE pair. Additionally, the phases of the LoS paths are modeled as independent and identically distributed (i.i.d.) random variables in each coherence block. We derive the phase aware MMSE, LMMSE, and LS channel estimators and obtain their statistics. In the UL, using the estimates for MR combining in the first layer, we compute closed-form UL achievable SE expressions for two-layer decoding scheme. In the DL, we obtain closed-form DL achievable SE expressions for both coherent and non-coherent transmission.

2. System model

A basebands OFDM system scheme with MIMO antennas is shown in Figure 1. Denote X_l ($l=0,1,2,\dots,N-1$), as modulated symbols on the transmitters of an OFDM subcarrier l th, assuming the independent, zero-mean random variables are supposed to have an average power σ^2 . You may write the complex OFDM baseband signal at IFFT output

$$x_n = \frac{1}{\sqrt{N}} \sum_{l=0}^{N-1} X_l e^{j2\pi nl/N}, n=0, \dots, N-1 \tag{1}$$

Where N is the total number of subcarriers in the OFDM frame and the length of the OFDM symbol is T seconds. The received OFDM signal on the receiver is combined with the oscillator signal on the local receiver, with the frequency offset being different from the signal received from the carrier's frequency due to the frequencies or the velocity of the Doppler. The signal received is sent is given by

$$y_n = (x_n \otimes h_n) e^{j2\pi n \Delta f T / N} + z_n \tag{2}$$

If h_n represents a channel impulsive response, the frequency offset of the received signal is $e^{j2\pi n \Delta f T / N}$ (Δf is the frequency offset of the received signal in sampling instants $\Delta f T$ is the frequency offset to the subcarrier frequency spacing ratio, and z_n is the AWGN, while \otimes is the denotation of the circular convolution. The receiver has a perfect time synchronization assuming a cyclic prefix is used. Note that a discrete Fourier transform (DFT) of the two-signal convolution in the time domain equals

the multiplication in frequency domain of the corresponding signals. Then the FFT output on the kth transmitter is generated by frequency domain signals

$$\begin{aligned}
 Y_k &= \sum_{l=0}^{N-1} X_l H_l S(l-k) + Z_k, k = 0, 1, 2, \dots, N-1 \quad \square \\
 &= X_k H_k S(0) + \sum_{l=0, l \neq k}^{N-1} X_l H_l S(l-k) + Z_k \quad (3)
 \end{aligned}$$

The first EQ (3) is a desirable data symbol and the second term is the ICI of unwanted data symbols generated by other OFDM sub-components. H_k is the pulsation response of the frequency-domain channel, and Z_k indicates the z_n frequency domain. The S(l-k) sequence is defined as the kth and lth subcarriers ICI coefficient which may be represented in Eq (4)

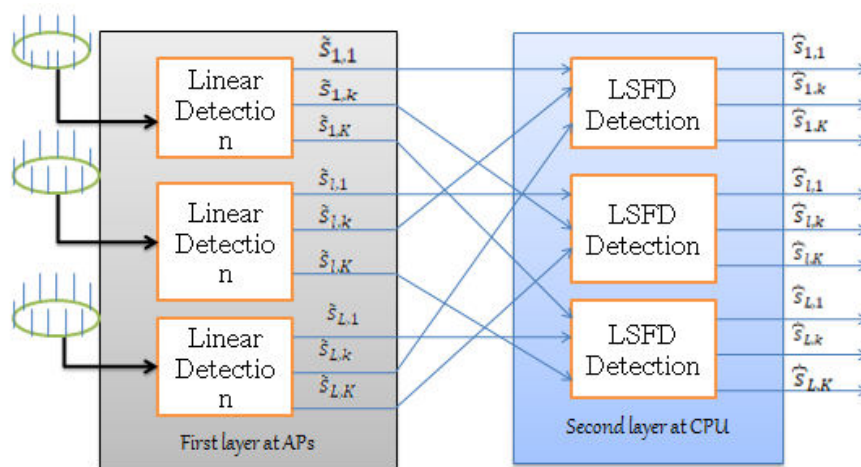


Figure 1: Massive MIMO architecture.

Now, as illustrated in Figure 1, the ICI Mitigation Scheme is exhibited in MIMO systems. The X_l modulated symbols (l=0,1,2, line,N-1) are space-time block coded by Alamouti (ASTBC). An antenna one is designated as the transmitted domain frequency signal on the lth transmitting subbrancher by A(1,l)=(X₀,0,0,x₀, alternatively,X_(N-2),0 for l=0,...,N-1, and by antenna two by A(2,l)=(0,X₁,0,X₀); If the CP is used, the receiver is synchronized perfectly. Also, the frequency offset is constant throughout the interval of two paths. The signal received by the time domain is indicated

$$y_n = (a_{1,n} \otimes h_{1,n} + a_{2,n} \otimes h_{2,n}) e^{\frac{j2\pi n \epsilon T}{N}} + z_n \quad (4)$$

Then a signal model of the principal route receiving the frequency-domain is represented as below.

$$Y_k = \sum_{l=0, l \neq k}^{N-1} A_{1,l} H_{1,l} S(1, l-k) + \sum_{l=0, l \neq k}^{N-1} A_{2,l} H_{2,l} S(2, l-k) + Z_k \quad (5)$$

The following can be summarized in the novel contributions of this chapter:

- New use of massive MIMO and RZF equalizer-based method for mitigation in combination.
- According to the authors' best knowledge, the technique was not employed for OFDM applications previously.
- A completely new MIMO system framework is proposed.

- We were primarily aiming at reducing the effect of ICI and mitigating the BER performance under deteriorating conditions and a delay in power profile not concentrated on previous research in this sector.

3. Proposed system

Massive MIMO (m-MIMO) is an extension of MIMO technology where we are deploying large number of antenna elements say tens to hundreds at the base station compared to User Terminals (UTs) served at the same time-frequency resource with no severe Inter-User-Interference.

- The adaptation of m-MIMO systems with the small cells is required to enhance the performance of data rates, channel capacity, power consumption, spectral efficiency, wireless devices connectivity with a huge amount of decrease in error rates and inference.
- Through Spatial Multiplexing, higher data rates can be achieved without growing the required spectrum band
- The base station estimates the reciprocal forward and reverse link channels with the use of Time division duplex (TDD) operation combined with reverse link pilots which achieves the perfect CSI.
- With the use of a large number of antennas, gain of antenna and directivity of radiating beam (signal) increases.
- For Uplink: Base Station needs to separate received signals from all the users
- For Downlink: There always exists some interference among the users (MUI) as BS sends the signal on the same channel
- By having CSI at AP or BS, BS knows about MUI. Thus, MUI can be mitigated by Intelligent Beam-forming i. e., Pre-coding technique.
- Pre-coder create beams that focus energy for each user by weighting the phase and amplitude of the antennas.
- We provide promising simulation results presenting how the spectral efficiency along with optimal energy efficiency to a great extent enhanced by combining massive MIMO and small cells; this is promising with both optimal pre-coding and low complexity beam-forming techniques.

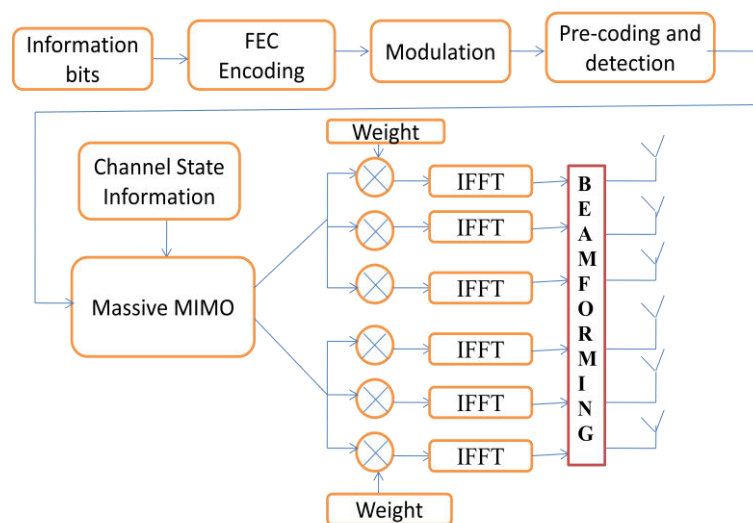


Figure 2: Block diagram of Transmitter

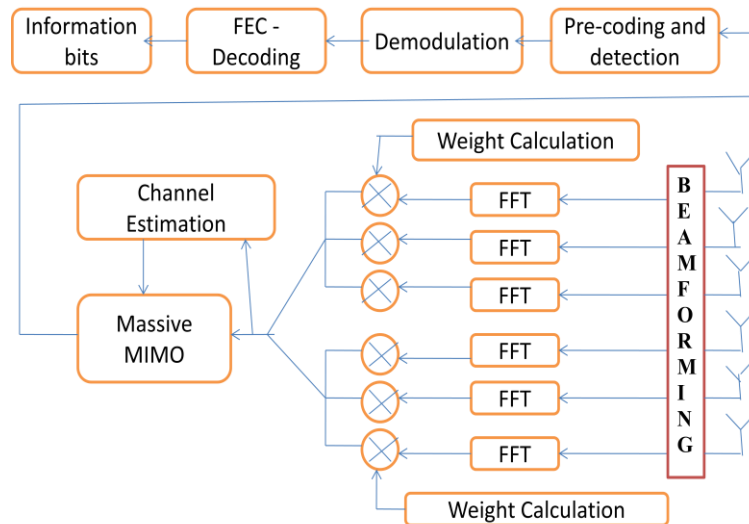


Figure 3: Block diagram of Receiver

3.1 System model

- Consider a solid microphone system consisting of a BS with M antennas and K users with a single set of antennas. Suppose every user's channel varies slowly, geographically, and flat.
- In this article, we explore a planner for optimising the spectrum efficiency of K users, together with a regularised pre-coder for zero forcing for QoS stress.
- Feedback is supposed to be received from all K users every time the BS schedules users. Each K user picks $[0]$ to quantify $[0]$ from a finite B -bit set, which is known to both the BS and all users as a code book and returns the codeword index that was picked.
- The scheduler uses the predicted SINR for the $(K \ M)$ possible combined channel matrices, $H[0]$ to choose M users from K users to optimise the sum rate.
- S is the chosen user set, containing user equipment and SCA base station power related information.

3.2 Algorithm

Step1: Under one m-MIMO system there exists multiple SCA's, which consists of K number of single antenna users are served by combination of antennas under SCA.

Step2: are frequency samples for data transmission generated from m-MIMO antenna

Step3: Operations of Scheduler

- Initially users are allocated to tier1 BSA when number of users or data rates are increasing scheduler jumps the users from tier1 to tier2
- Again, when users are decreasing it returns back the users to tier1.
- When users are more SE is improved and when users are less EE is improved which means power consumption is reduced
- To achieve this scheduler is introduces a concept called power splitting, where power consumed by the subcarrier is spitted into Dynamic Power and Static Power.

- Dynamic power is generated between tier2 antennas and UE which is always dynamic in nature in terms of adding and removing of users from tier2

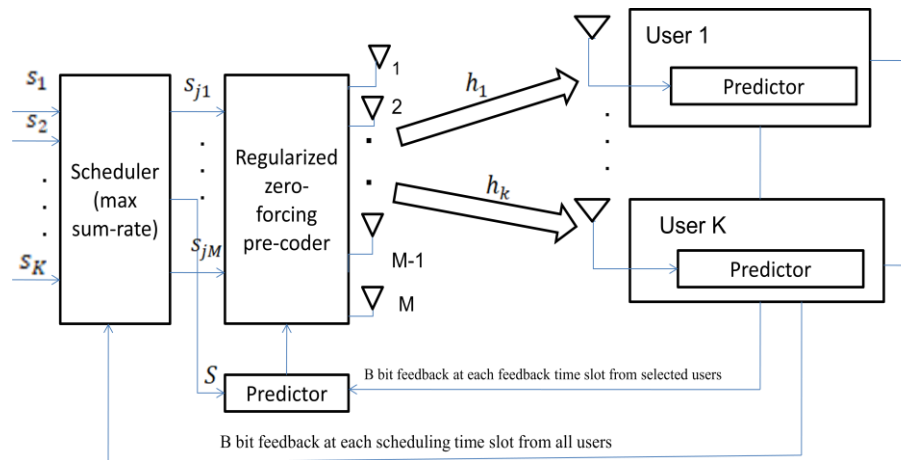


Figure 4: Operation of Regularized Zero forcing pre-coder with Massive MIMO system

- Whereas static power is calculated between tier1 to BSs in SCA which are nothing but fixed number of equipment's like routers placed in SCA.
- By calculating these powers, the jumping of users between the tiers is possible.
- They are frequency allocated version of S generated from Scheduler

Step 4: Predictor operation

- Predictor is used to predict beforehand about the power consumption of increased or decreased users which allows transmitting signals perfectly without interrupting the existing users.
- It also calculated the spectrum required for increased users and SCAs

Step5: These predicted values are given to RZF block where actual processing is done.

Step6: Operations of RZF

- Linear Pre-coding technique. It receives the data from each transmitting antenna through the scheduler.
- Receives the information from predictor to generate the perfect optimization values of static and dynamic power consumptions and improves the SE.
- First it will calculate the channel impulse response H matrix where received signal gain is calculated
- If the gain is weak MMSE equalizers are used to reduce the ISI and BER which in turn increase the gain of the signal.

Step7: Predictor at UE calculates SE levels, data rate, power consumption and these are fed back to the predictor at BS in SCA to adjust the parameters accordingly.

Step8: With this we can achieve SE, EE, and increased data rates.

3.3. RZFequalizer

To solve for x , we know that we need to find a matrix W which satisfies $WH=I$. Let us now try to understand the math for extracting the two symbols which interfered with each other. The RZFApproach tries to find a coefficient W which minimizes the criterion,

$$E\{[Wy - x][Wy - x]^H\}$$

Solving the above equation,

$$W = [H^H H + N_0 I]^{-1} H^H$$

$$H^H H = \begin{bmatrix} h_{1,1}^* & h_{2,1}^* \\ h_{1,2}^* & h_{2,2}^* \end{bmatrix} \begin{bmatrix} h_{1,1} & h_{1,2} \\ h_{2,1} & h_{2,2} \end{bmatrix}$$

$$= \begin{bmatrix} |h_{1,1}|^2 + |h_{2,1}|^2 & h_{1,1}^* h_{1,2} + h_{2,1}^* h_{2,2} \\ h_{1,2}^* h_{1,1} + h_{2,2}^* h_{2,1} & |h_{1,2}|^2 + |h_{2,2}|^2 \end{bmatrix}$$

Finally, the receiver can obtain an estimate of the two transmitted symbols x_1, x_2 i.e.,

$$\begin{bmatrix} x_1 \\ x_2 \end{bmatrix} = (H^H H + N_0 I)^{-1} H^H \begin{bmatrix} y_{1,1} \\ y_{1,2} \\ y_{2,1}^* \\ y_{2,2}^* \end{bmatrix}$$

4. Simulation results

This section gives the detailed analysis of simulations which are implemented by using MATLAB R 2016a.

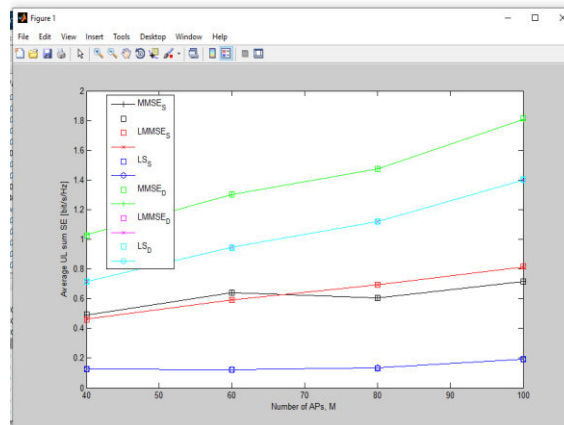


Figure 5: Proposed scalable massive MIMO system with MMSE, LMMSE and LS estimations with 100 number of access points.

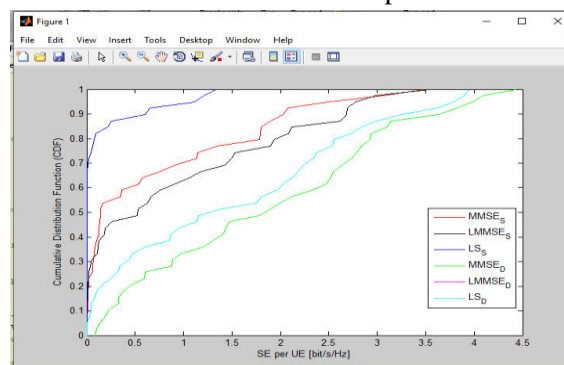


Figure 6: SE of proposed scalable massive MIMO system with MMSE, LMMSE and LS estimations in uplink.

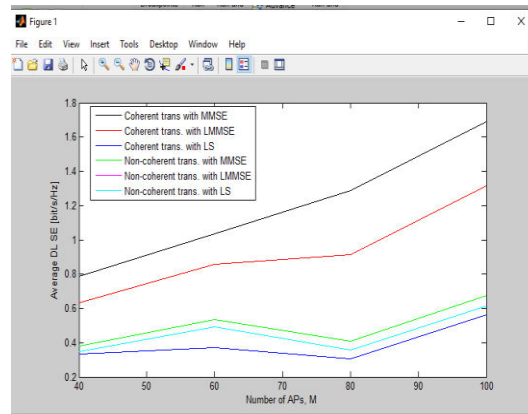


Figure 7: Proposed scalable massive MIMO system with MMSE, LMMSE and LS estimations with coherent and non-coherent transmissions

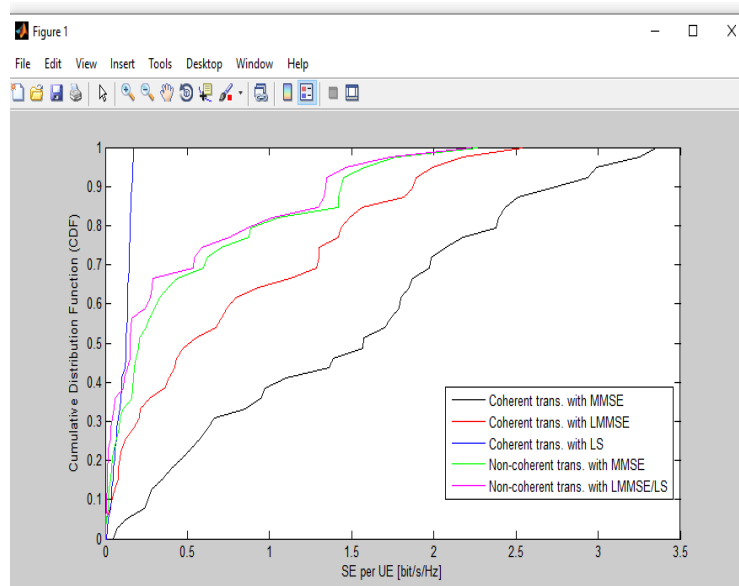


Figure 8: CDF of proposed scalable massive MIMO system with MMSE, LMMSE and LS estimations with coherent and non-coherent transmissions

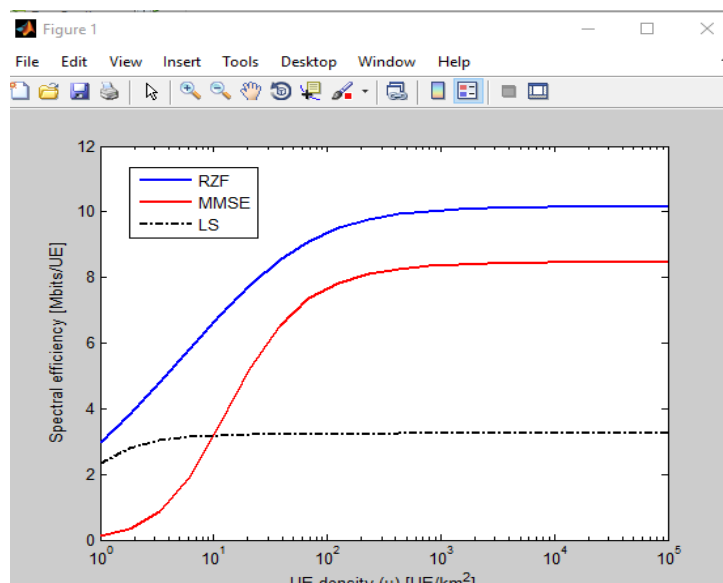


Figure 9: Spectral efficiency Vs User density of all schemes

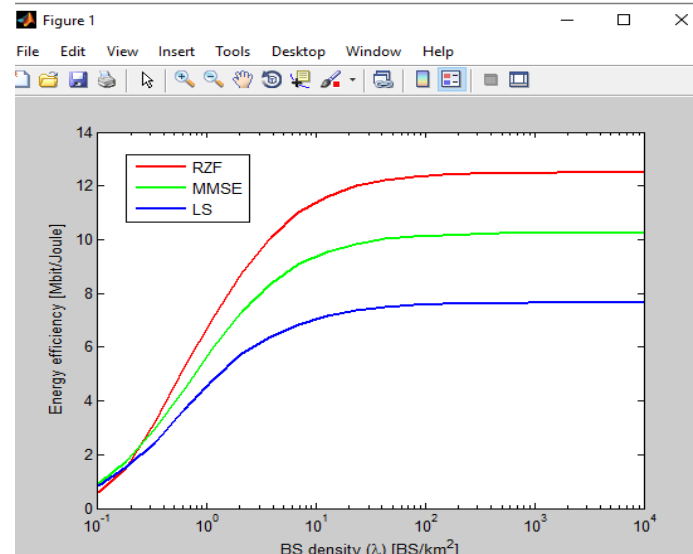


Figure 10: Energy Efficiency Vs BS density

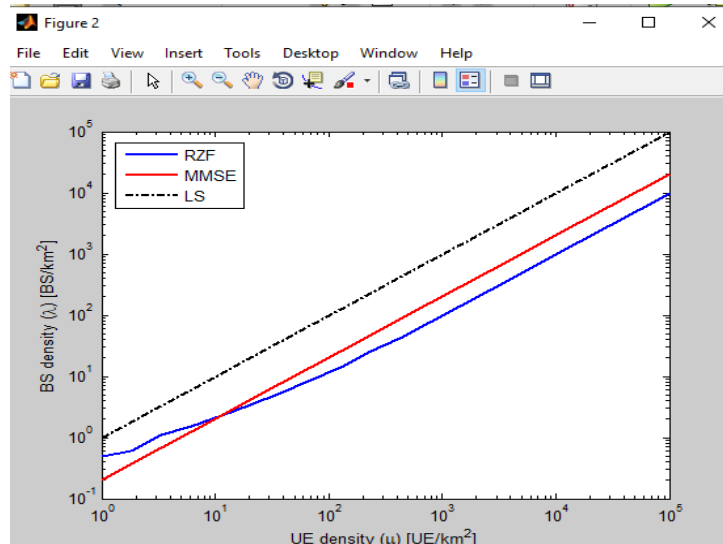


Figure 11: BS density vs UE density

5. Conclusion

This chapter described the effectiveness of Massive MIMO system with the enhancement of CIR in presence of AWGN and frequency selective Rayleigh fading channel. A combined scheme of RZF equalizer-based ICI mitigation approach is employed for enhancing the performance of Massive MIMO system. In addition, this algorithm reduced the complexity and processing delay by improving BER performance of Massive MIMO system. However, the weights utilized in CIR expression are not optimal and further there is a lack of translation invariance. Thus, it is required to address these issues to maximize the performance of Massive MIMO system for 5G wireless networks.

References

[1]. Björnson, Emil, and Luca Sanguinetti. "Power scaling laws and near-field behaviors of massive MIMO and intelligent reflecting surfaces." *IEEE Open Journal of the Communications Society* 1 (2020): 1306-1324.

- [2]. Chataut, Robin, and Robert Akl. "Massive MIMO systems for 5G and beyond networks—overview, recent trends, challenges, and future research direction." *Sensors* 20.10 (2020): 2753.
- [3]. You, Li, et al. "Massive MIMO transmission for LEO satellite communications." *IEEE Journal on Selected Areas in Communications* 38.8 (2020): 1851-1865.
- [4]. Ma, X., & Gao, Z. (2020). Data-driven deep learning to design pilot and channel estimator for massive MIMO. *IEEE Transactions on Vehicular Technology*, 69(5), 5677-5682.
- [5]. Elbir, A. M., Papazafeiropoulos, A., Kourtessis, P., & Chatzinotas, S. (2020). Deep channel learning for large intelligent surfaces aided mm-wave massive MIMO systems. *IEEE Wireless Communications Letters*, 9(9), 1447-1451.
- [6]. Gunnarsson, Sara, Jose Flordelis, Liesbet Van der Perre, and Fredrik Tufvesson. "Channel hardening in massive MIMO: Model parameters and experimental assessment." *IEEE Open Journal of the Communications Society* 1 (2020): 501-512.
- [7]. Chen, S., Zhang, J., Björnson, E., Zhang, J., & Ai, B. (2020). Structured massive access for scalable cell-free massive MIMO systems. *IEEE Journal on Selected Areas in Communications*, 39(4), 1086-1100.
- [8]. Ren, Hong, et al. "Joint pilot and payload power allocation for massive-MIMO-enabled URLLC IIoT networks." *IEEE Journal on Selected Areas in Communications* 38.5 (2020): 816-830.
- [9]. Ahmed, A. H., Al-Heety, A. T., Al-Khateeb, B., & Mohammed, A. H. (2020, June). Energy Efficiency in 5G Massive MIMO for Mobile Wireless Network. In *2020 International Congress on Human-Computer Interaction, Optimization and Robotic Applications (HORA)* (pp. 1-6). IEEE.
- [10]. Ke, Malong, Zhen Gao, Yongpeng Wu, Xiqi Gao, and Kai-Kit Wong. "Massive access in cell-free massive MIMO-based Internet of Things: Cloud computing and edge computing paradigms." *IEEE Journal on Selected Areas in Communications* 39, no. 3 (2020): 756-772.
- [11]. Elbir, Ahmet M., and Sinem Coleri. "Federated learning for channel estimation in conventional and IRS-assisted massive MIMO." *arXiv preprint arXiv:2008.10846* (2020).
- [12]. Shlezinger, Nir, et al. "Dynamic metasurface antennas for 6G extreme massive MIMO communications." *IEEE Wireless Communications* 28.2 (2021): 106-113.
- [13]. Ye, H., Gao, F., Qian, J., Wang, H., & Li, G. Y. (2020). Deep learning-based denoise network for CSI feedback in FDD massive MIMO systems. *IEEE Communications Letters*, 24(8), 1742-1746.
- [14]. Zhao, R., Woodford, T., Wei, T., Qian, K., & Zhang, X. (2020, April). M-cube: A millimeter-wave massive MIMO software radio. In *Proceedings of the 26th Annual International Conference on Mobile Computing and Networking* (pp. 1-14).
- [15]. Ying, K., Gao, Z., Lyu, S., Wu, Y., Wang, H., & Alouini, M. S. (2020). GMD-based hybrid beamforming for large reconfigurable intelligent surface assisted millimeter-wave massive MIMO. *IEEE Access*, 8, 19530-19539.
- [16]. Björnson, E., & Sanguinetti, L. (2020). Scalable cell-free massive MIMO systems. *IEEE Transactions on Communications*, 68(7), 4247-4261.
- [17]. Demir, Ö. T., Björnson, E., & Sanguinetti, L. (2021). Foundations of user-centric cell-free massive MIMO. *arXiv preprint arXiv:2108.02541*.

- [18]. Angeletti, Piero, and Riccardo De Gaudenzi. "A pragmatic approach to massive MIMO for broadband communication satellites." *IEEE Access* 8 (2020): 132212-132236.
- [19]. Ma, Wenyan, et al. "Sparse channel estimation and hybrid precoding using deep learning for millimeter wave massive MIMO." *IEEE Transactions on Communications* 68.5 (2020): 2838-2849.
- [20]. Guo, Jiajia, Chao-Kai Wen, and Shi Jin. "Deep learning-based CSI feedback for beamforming in single-and multi-cell massive MIMO systems." *IEEE Journal on Selected Areas in Communications* (2020).
- [21]. Vu, T. T., Ngo, D. T., Tran, N. H., Ngo, H. Q., Dao, M. N., & Middleton, R. H. (2020). Cell-free massive MIMO for wireless federated learning. *IEEE Transactions on Wireless Communications*, 19(10), 6377-6392.
- [22]. You, L., Xiong, J., Zappone, A., Wang, W., & Gao, X. (2020). Spectral efficiency and energy efficiency tradeoff in massive MIMO downlink transmission with statistical CSIT. *IEEE Transactions on Signal Processing*, 68, 2645-2659.
- [23]. de Sena, A. S., Lima, F. R. M., da Costa, D. B., Ding, Z., Nardelli, P. H., Dias, U. S., & Papadias, C. B. (2020). Massive MIMO-NOMA networks with imperfect SIC: Design and fairness enhancement. *IEEE Transactions on Wireless Communications*, 19(9), 6100-6115.
- [24]. Liang, P., Fan, J., Shen, W., Qin, Z., & Li, G. Y. (2020). Deep learning and compressive sensing-based CSI feedback in FDD massive MIMO systems. *IEEE Transactions on Vehicular Technology*, 69(8), 9217-9222.
- [25]. Guo, J., Yang, X., Wen, C. K., Jin, S., & Li, G. Y. (2020). DL-based CSI feedback and cooperative recovery in massive MIMO. *arXiv preprint arXiv:2003.03303*.